

June, 2002

OU-HET 414

hep-ph/0206207

Exploring the neutrino mass matrix at M_R scale

Takahiro Miura^{*}, Tetsuo Shindou[†] and Eiichi Takasugi[‡]

Department of Physics, Osaka University

Toyonaka, Osaka 560-0043, Japan

Abstract

We discuss the neutrino mass matrix which predicts zero or small values of $|V_{13}|$ and found the inequality, $\sin^2 2\theta_{12} \leq \sin^2 2\theta_{\odot}$, where $\sin^2 2\theta_{12}$ is the mixing angle at M_R scale and $\sin^2 2\theta_{\odot}$ is the value determined by the solar neutrino oscillation. This constraint says that the model which predicts a larger value of $\tan^2 \theta_{12}$ at M_R than the experimental value is excluded. In particular, the bi-maximal mixing scheme at M_R scale is excluded, from the experimental value $\tan^2 \theta_{\odot} < 1$. In this model, $|V_{13}|$ and a Dirac phase at m_Z are induced radiatively and turn out to be not small. The effective neutrino mass $\langle m_{\nu} \rangle$ is expected to be of order 0.05 eV.

^{*} e-mail address: miura@het.phys.sci.osaka-u.ac.jp

[†] e-mail address: shindou@het.phys.sci.osaka-u.ac.jp

[‡] e-mail address: takasugi@het.phys.sci.osaka-u.ac.jp

1. INTRODUCTION

The SuperKamiokande data has discovered the neutrino mixing between ν_μ and ν_τ from the atmospheric data[1]. Now the SNO data[2] together with SuperKamiokande data[3] have solved the solar neutrino puzzle and pinpointed a solution among four solutions. That is, its origin is the ν_e and ν_μ mixing and the LMA solution is the most probable one. They are summarized as

$$\begin{aligned}\tan^2 \theta_\odot &\simeq 0.34, & \Delta m_\odot^2 &\simeq 5 \times 10^{-5} \text{ eV}^2, \\ \sin^2 2\theta_{\text{atm}} &\simeq 1, & \Delta m_{\text{atm}}^2 &\simeq 3 \times 10^{-3} \text{ eV}^2,\end{aligned}\tag{1}$$

where θ_\odot and θ_{atm} are mixing angles which appear in the solar and atmospheric neutrino oscillations, and in effect are mixing angles between the 1st and the 2nd and between the 2nd and the 3rd mass eigenstates, respectively. Δm_\odot^2 and Δm_{atm}^2 are the squared mass differences defined by $\Delta m_\odot^2 = m_2^2 - m_1^2$ and $\Delta m_{\text{atm}}^2 = |m_3^2 - m_2^2|$, where m_i is the mass of the i -th mass eigenstate of neutrinos. Usually, the sign convention, $\Delta m_\odot^2 = m_2^2 - m_1^2 > 0$ is taken, in which case the result from the SNO-SuperKamiokande data[2, 3] favors the normal side, $\tan^2 \theta_\odot < 1$, and disfavors the dark side, $\tan^2 \theta_\odot > 1$ [4]. Another important information from the CHOOZ data[5] gives a severe upper limit for $|V_{13}|$

$$|V_{13}| < 0.16, \tag{2}$$

where V_{13} is the element of the MNS neutrino mixing matrix[6] representing the mixing between the 1st and the 3rd mass eigenstates. If we combine these information, the neutrino mixing matrix is approximately written by

$$V = \begin{pmatrix} c_\odot & -s_\odot & 0 \\ s_\odot c_{\text{atm}} & c_\odot c_{\text{atm}} & -s_{\text{atm}} \\ s_\odot s_{\text{atm}} & c_\odot s_{\text{atm}} & c_{\text{atm}} \end{pmatrix} \begin{pmatrix} 1 & & \\ & e^{i\alpha_M} & \\ & & e^{i\beta_M} \end{pmatrix}, \tag{3}$$

where we included two Majorana CP violation phases[7, 8, 9] in the mixing matrix which play an important role for the neutrinoless double beta decay[8].

Among the above experimental information, the most mysterious point is the puzzle why $|V_{13}|$ is so small in comparison with other mixing angles, θ_\odot and θ_{atm} . If it is really

small, we have to find out the reason for it. For a small quantity at the low energy scale, the naturalness usually asserts that it is zero at the higher energy scale, because it is quite hard to reproduce such a small quantity at the low energy scale.

In this paper, we consider a possibility that $|V_{13}| = 0$ at the energy scale where the left-handed neutrino mass is induced by the see-saw mechanism. There are many advantages to consider this possibility. (1) The small value of $|V_{13}|$ is naturally explained because it is induced by the radiative correction. (2) This scenario may be realized in some theoretical models at M_R scale[10, 11, 12, 13]. (3) The Dirac CP violation phase is induced by the radiative correction.

Now, we consider the neutrino mass matrix which predicts $|V_{13}| = 0$ at M_R scale, in the diagonal basis of the charged lepton mass matrix. This mass matrix contains only seven parameters, three neutrino masses, two mixing angles and two Majorana CP violation phases, and thus there is no Dirac CP violation phase at M_R scale. This may give an possibility that the Dirac CP violation phase which appears in the neutrino oscillation may be related to Majorana CP violation phases, which may be related in the leptogenesis, since in our model, two Majorana phases are associated with phases of neutrino masses and they may well have some relation with phases from the heavy right-handed Majorana mass matrix.

This paper is organized as follows: In Section 2, we explain our model and the framework of neutrino mass matrix. The radiative correction is taken into account and the mass matrix is diagonalized analytically to connect the parameters at M_R scale and the present experimental scale, m_Z . In Section 3, the general feature of our result is explained and the predictions are given. In Section 4, by using analytic result, numerical analysis is made on the induced size of $|V_{13}|$, the Dirac CP violation phase, δ , and the effective mass of the neutrinoless double beta decay. The discussion on the absolute size of neutrino mass is given. Summary and discussions are given in Section 5.

2. THE MODEL

We consider a class of left-handed neutrino mass matrices which gives $V_{13} = 0$, where V is the neutrino mixing matrix. We assume that this mass matrix is derived by the see-saw mechanism according to the SUSY GUT scenario at the right-handed neutrino mass, M_R scale and evolves following the renormalization equation for MSSM to the Z boson mass scale, m_Z . In this model, V_{13} at m_Z scale is induced by radiative correction. We examine the size of V_{13} , the Dirac CP violation phase, δ , Majorana CP violation phases, α_M and β_M , and the effective mass of the neutrinoless double beta decay, $\langle m_\nu \rangle$.

(a) The mass matrix at M_R

The mass matrix which gives $V_{13} = 0$ is generally expressed in the diagonal basis of the charged lepton mass matrix as

$$m_\nu(M_R) = O D_\nu O^T, \quad (4)$$

where

$$D_\nu = \text{diag}(M_1, M_2 e^{i\alpha_0}, M_3 e^{i\beta_0}), \quad (5)$$

with Majorana phases, α_0 and β_0 . O is the mixing matrix at M_R scale and is given by

$$O = \begin{pmatrix} 1 & 0 & 0 \\ 0 & c_{23} & -s_{23} \\ 0 & s_{23} & c_{23} \end{pmatrix} \begin{pmatrix} c_{12} & -s_{12} & 0 \\ s_{12} & c_{12} & 0 \\ 0 & 0 & 1 \end{pmatrix}. \quad (6)$$

with $c_{ij} = \cos \theta_{ij}$ and $s_{ij} = \sin \theta_{ij}$. In the following, we use θ_{ij} only as an angle at M_R scale.

(b) The neutrino mass matrix at m_Z

The neutrino mass matrix at m_Z is given by[14]

$$m_\nu(m_Z) = \text{diag}(1, 1, \alpha) O D_\nu O^T \text{diag}(1, 1, \alpha), \quad (7)$$

where α is defined by

$$\alpha \equiv 1 - \epsilon = 1/\sqrt{I_\tau} = \left(\frac{m_Z}{M_R} \right)^{\frac{1}{8\pi^2}(1+\tan^2 \beta)(m_\tau/v)^2} < 1. \quad (8)$$

Here m_τ is the τ lepton mass, $v^2 = v_u^2 + v_d^2$ and $\tan \beta = v_u/v_d$ with v_i being the vacuum expectation value of MSSM Higgs doublet $\langle H_i \rangle (i = u, d)$.

In order to estimate ϵ , we assume the right-handed mass scale, M_R and the region of $\tan \beta$ as

$$M_R = 10^{13}(\text{GeV}) , \quad 2 < \tan \beta < 50 . \quad (9)$$

Then, with $m_Z = 91.187(\text{GeV})$, $m_\tau = 1.777(\text{GeV})$ and $v = 245.4(\text{GeV})$, we find

$$8 \times 10^{-4} < \epsilon < 5 \times 10^{-2} . \quad (10)$$

(c) Masses and the mixing matrix at m_Z

The effect of the radiative correction to neutrino mass matrix has been discussed by many authors[14, 15, 16] and the following is known. (1) The mixing angles are stable for the case of the hierarchical or the inverted-hierarchical neutrino mass scheme, $m_1 \ll m_2 \ll m_3$ or $m_3 \ll m_1 \ll m_2$. (2) The instability occurs for $m_1 \simeq m_2$. (3) The Majorana phases in neutrino masses may play an important role[16].

Since the stable case is well analyzed, we focus on the unstable case. That is, we consider the following mass relation holds at M_R scale,

$$\begin{aligned} M_1 &\simeq M_2 , \quad 0 < \Delta_{21} \ll |\Delta_{31}| , \\ 0 < \Delta_{21} &\ll M_1^2 , \quad \epsilon M_1^2 \simeq \epsilon M_2^2 \ll |\Delta_{31}| , \end{aligned} \quad (11)$$

where $\Delta_{21} = M_2^2 - M_1^2$, $\Delta_{31} = M_3^2 - M_1^2$ and we chose the convention, $\Delta_{21} > 0$. The diagonalization of the neutrino mass matrix is made analytically and the derivation is given in Appendix.

In the following, we summarize the result derived in Appendix. As for neutrino masses themselves, corrections are small and of order ϵM_i , because we are considering the situation where $M_1^2 \simeq M_2^2 \gg \Delta_{21} \sim \epsilon M_2^2$. Thus, neutrino masses at M_R and m_Z can be considered to be the same.

$$m_i \simeq M_i . \quad (12)$$

The radiative correction gives effect to the mass difference between m_1 and m_2 ,

$$\Delta m_\odot^2 = m_2^2 - m_1^2 = \frac{\Delta_{21} - 4\epsilon m_1^2 s_{\text{atm}}^2 \cos 2\theta_{12}}{\cos 2\theta} > 0 , \quad (13)$$

while the mass difference between the 2nd and the 3rd receives only a negligible effect, so that

$$\Delta m_{\text{atm}}^2 = m_3^2 - m_2^2 \simeq m_3^2 - m_1^2 \simeq \Delta_{31} . \quad (14)$$

In the above, we required $\Delta m_{\odot}^2 > 0$ in accordance with the common experimental analysis which gives $\tan^2 \theta_{\odot} = 0.34 < 1$. As for mixing angles, the radiative correction does not give any effect to the mixing between the 2nd and the 3rd mass eigenstates either. That is,

$$\theta_{\text{atm}} = \theta_{23} . \quad (15)$$

Thus, in the following, we use m_i for M_i except for the discussion of the mass difference and θ_{atm} for θ_{23} in order to express θ_{\odot} , $|V_{13}|$, δ , α_M and β_M in terms of observables at the low energy as possible as we can.

The MNS mixing matrix which is given in Eq. (A.15) is expressed as

$$V = \begin{pmatrix} c_{\odot} & -s_{\odot} & -|V_{13}|e^{-i\delta} \\ s_{\odot}c_{\text{atm}} & c_{\odot}c_{\text{atm}} & -s_{\text{atm}} \\ s_{\odot}s_{\text{atm}} & c_{\odot}s_{\text{atm}} & c_{\text{atm}} \end{pmatrix} \begin{pmatrix} 1 & & \\ & e^{i\alpha_M} & \\ & & e^{i\beta_M} \end{pmatrix} , \quad (16)$$

where $\theta_{\text{atm}} = \theta_{23}$, θ_{\odot} is

$$\begin{aligned} s_{\odot} &= |s_{12}c + c_{12}se^{i\alpha_0/2}| , \\ c_{\odot} &= |c_{12}c - s_{12}se^{-i\alpha_0/2}| , \end{aligned} \quad (17)$$

with θ defined by

$$\sin 2\theta = \frac{4\epsilon m_1^2 s_{\text{atm}}^2 \sin 2\theta_{12} \cos \frac{\alpha_0}{2}}{\Delta m_{\odot}^2} . \quad (18)$$

The induced mixing element, $|V_{13}|$ is given by

$$|V_{13}| = \frac{\epsilon m_1 m_3 \sin 2\theta_{12} \sin 2\theta_{\text{atm}} \sin \frac{\alpha_0}{2}}{\Delta m_{\text{atm}}^2} . \quad (19)$$

A Dirac CP violation phase, δ , and two Majorana CP violating phases, α_M and β_M are

$$\begin{aligned} \delta &= \xi_1 + \xi_2 - \frac{\pi}{2} + \frac{\alpha_0}{2} - \beta_0 , \\ \alpha_M &= \xi_2 - \xi_1 - \frac{\alpha_0}{2} , \\ \beta_M &= \xi_2 - \frac{\beta_0}{2} , \end{aligned} \quad (20)$$

with

$$\begin{aligned}\xi_1 &= \arg(c_{12}c - s_{12}se^{-i\alpha_0/2}) , \\ \xi_2 &= \arg(s_{12}c + c_{12}se^{i\alpha_0/2}) .\end{aligned}\tag{21}$$

In the mixing matrix, θ_{12} and two Majorana phases, α_0 and β_0 are only parameters defined at M_R . All other parameters are expressed by physical quantities at m_Z .

3. GENERAL FEATURES

As we explained, we take the convention $\Delta m_\odot^2 > 0$ for which the result from the SNO-SuperKamiokande data requires that the mixing angle should be in the normal side, $\tan^2 \theta_\odot = 0.34 < 1$ [2, 3]. Also we take the convention, $\Delta_{21} = M_2^2 - M_1^2 > 0$.

(a) The solar mixing angle

Here, we discuss the relation between θ_{12} defined at M_R scale and θ_\odot defined at m_Z , the value from the solar neutrino oscillation data. We parametrize the solar neutrino mixing angle as

$$\tan^2 \theta_\odot = \frac{1-p}{1+p} , \quad \text{or} \quad \sin^2 2\theta_\odot = 1 - p^2 ,\tag{22}$$

and then $p > 0$ is required to guarantee $\tan^2 \theta_\odot < 1$. From Eq. (17), p is given by

$$\begin{aligned}p &= \cos 2\theta_{12} \cos 2\theta - \sin 2\theta_{12} \sin 2\theta \cos \frac{\alpha_0}{2} \\ &= \cos 2\theta_{12} \cos 2\theta - 2h \sin^2 2\theta_{12} \cos^2 \frac{\alpha_0}{2} ,\end{aligned}\tag{23}$$

where we used $\sin 2\theta$ defined in Eq. (18) to derive the second line and we defined the positive quantity h to avoid the complexity of equation,

$$h = \frac{2\epsilon m_1^2 s_{\text{atm}}^2}{\Delta m_\odot^2} .\tag{24}$$

From $p > 0$ together with $h > 0$, we find $\cos 2\theta_{12} \cos 2\theta > 0$. Now we look carefully the equation for $\Delta m_\odot^2 > 0$ in Eq. (13). With $\Delta_{21} > 0$ together with the above condition, only consistent choice is

$$\cos 2\theta_{12} > 0 , \quad \cos 2\theta > 0 .\tag{25}$$

Now that the sign of $\cos 2\theta$ is fixed to be positive, we can eliminate $\cos 2\theta$ in Eq. (23).

Thus, we can express $\tan^2 \theta_\odot$ in terms of θ_{12} , α_0 and h ,

$$\frac{1 - \tan^2 \theta_\odot}{1 + \tan^2 \theta_\odot} = \cos 2\theta_{12} \sqrt{1 - 4h^2 \sin^2 2\theta_{12} \cos^2 \frac{\alpha_0}{2}} - 2h \sin^2 2\theta_{12} \cos^2 \frac{\alpha_0}{2}. \quad (26)$$

This is the equation which relates the angle θ_{12} at M_R scale and the solar mixing angle, θ_\odot .

Next, we solve the above equation with respect to $\cos \alpha_0$ and find

$$1 + \cos \alpha_0 = \frac{1}{h \sin^2 2\theta_{12}} \left(-|\cos 2\theta_\odot| - h \cos^2 2\theta_{12} + \cos 2\theta_{12} \sqrt{h^2 \cos^2 2\theta_{12} + 2|\cos 2\theta_\odot| h + 1} \right) \quad (27)$$

By requiring $0 \leq 1 + \cos \alpha \leq 2$, we obtain

$$\frac{\sin^2 2\theta_\odot}{\sin^2 2\theta_\odot + (|\cos 2\theta_\odot| + 4\epsilon s_{\text{atm}}^2 (m_1^2 / \Delta m_\odot^2))^2} \leq \sin^2 2\theta_{12} \leq \sin^2 2\theta_\odot, \quad (28)$$

where we used the expression of h in Eq. (24). This inequality shows the region of $\sin^2 2\theta_{12}$ at M_R where the experimental value $\sin^2 2\theta_\odot$ at m_Z is realized.

Before discussing the meaning of these equations, it should be mentioned that the above result is valid as far as $|V_{13}(M_R)| \ll |\sin \theta_{12}|$ is satisfied, where $\sin \theta_{12}$ and $|V_{13}(M_R)|$ are quantities at M_R scale.

Now we discuss the meaning of the inequality. Firstly, we comment that the equality $\sin^2 2\theta_{12} = \sin^2 2\theta_\odot$ (stable case) holds in several cases, (1) the hierarchical mass case, $m_1 \ll m_2$, where $m_2^2 \simeq \Delta m_\odot^2$, (2) the small ϵ case which corresponds to the small $\tan \beta$, (3) the special case, $\alpha_0 = \pi$, even with $m_1^2 \simeq m_2^2 \gg \Delta m_\odot^2$.

One of the most important observation will be the following: The inequality $\sin^2 2\theta_{12} \leq \sin^2 2\theta_\odot$ holds for most of models, because physically feasible models have to predict small values of $|V_{13}|$. Thus, we can generally say that the model which constructed at higher energy scale such as M_R must have $\tan^2 \theta_{12}$ less than or equal to the experimental value, $\tan^2 \theta_\odot = 0.34$. The bi-maximal mixing scheme which is realized at M_R is not acceptable from the present experimental data. This may give a big obstacle for model building, because the model should predicts the experimental angle which does not have any particular meaning in the stable angle case. On the other hand, for the unstable case, the model needs to predict smaller value at M_R and the radiative correction lifts

the value to the experimental one, by the interplay among neutrino mass, $\tan \beta$ and the CP violation angle, α_0 .

(b) The size of the induced $|V_{13}|$

The induced $|V_{13}|$ is given in Eq. (19). Since it is proportional to $\epsilon(m_1 m_3 / \Delta m_{\text{atm}}^2)$, its value is suppressed by $\Delta m_{\odot}^2 / \Delta m_{\text{atm}}^2$, in comparison with corrections to the mass squared difference for the solar neutrino mixing and the solar neutrino angle. If $m_3 / m_1 > 1$, some enhancement is expected.

(c) The CP violation angles

The Dirac CP violation phase, δ is induced from two Majorana phases. Since α_0 is deeply involved in determining the solar mixing angle, δ aside from β_0 can be determined. Thus, we define

$$\delta_1 = \delta + \beta_0 = \xi_1 + \xi_2 - \frac{\pi}{2} + \frac{\alpha_0}{2}, \quad (29)$$

for which we analyze numerically in the next section. We hope that the knowledge of the phase β_0 may be derived from the information from the leptogenesis.

(d) Neutrinoless double beta decay

With $m_1 \simeq m_2$, the effective neutrino mass for the neutrinoless double beta decay in this mode is simply given by

$$\begin{aligned} \langle m_\nu \rangle &\equiv \left| \sum_j m_j V_{1j}^2 \right| \\ &\simeq m_1 \left| (c_{12}c - s_{12}s e^{-i\alpha_0/2})^2 + (s_{12}c + c_{12}s e^{i\alpha_0/2})^2 e^{-i\alpha_0} \right| \\ &= m_1 \sqrt{1 - \sin^2 2\theta_{12} \sin^2 \frac{\alpha_0}{2}}, \end{aligned} \quad (30)$$

where we neglect $m_3 V_{13}^2$, because $|V_{13}|$ is small.

4. NUMERICAL ANALYSIS

In the following, we confine the region of α_0 to be $0 \leq \alpha_0 \leq \pi$. Most of physical quantities do not receive the effect if we extend its region to $-\pi \leq \alpha_0 \leq \pi$ except for the sign change of the Dirac phase.

The radiative correction is proportional to ϵ , which is a rapidly increasing function of $\tan \beta$ as seen in Eq. (8). Therefore, the effect is smaller for smaller value of $\tan \beta$. In the following, we consider two cases, $\tan \beta = 50$ and $\tan \beta = 20$. For the numerical analysis, we use the experimental data given in Eq. (1).

(a) The angle $\sin^2 2\theta_{12}$

As we see from Eq. (26), the solar angle is determined by a Majorana phase α_0 , the neutrino mass m_1 and the mixing angle $\sin^2 2\theta_{12}$ at M_R scale. Therefore, when we give the value of $\sin^2 2\theta_\odot$, three parameters are constrained and the contour curve for a given α_0 is drawn. In Fig. 1, the contour plot of α_0 in the $\sin^2 2\theta_{12}$ and m_1 plain is shown for $\tan \beta = 50$ with $\tan^2 \theta_\odot = 0.34$. The wide values of $\sin^2 2\theta_{12}$ are allowed which may be seen from Eq. (28).

A particular feature is that the most of region corresponds to $\pi/2 \leq \alpha_0 \leq \pi$. That is, if we choose the value of α_0 in this region, almost any value of $\sin^2 2\theta_{12}$ at M_R scale can reproduce the experimental solar angle with an appropriate choice of m_1 , which should be greater than, say, 0.02 eV. If the mass $m_1 < 0.01$ eV, the $\sin^2 2\theta_{12}$ is stable and should reproduce the solar angle precisely at M_R scale.

(b) The induced value of $|V_{13}|$

As we see from Eq. (19), $|V_{13}|$ depends on four parameters, α_0 , m_1 , m_3 and $\sin^2 2\theta_{12}$. Therefore, we define $|V_{13}|(m_1/m_3)$ and give the contour plot in Fig. 2 for $\tan \beta = 50$. From Fig. 1, we know that the most of the region corresponds to $\pi/2 \leq \alpha_0 \leq \pi$. Thus, the point moves to the upper right corner in $\sin^2 2\theta_{12}$ and m_1 plain, α_0 approaches to $\sim \pi$ from $\pi/2$ and both $\sin^2 2\theta_{12}$ and m_1 increase. Since $|V_{13}|(m_1/m_3)$ is proportional to $m_1^2 \sin 2\theta_{12} \sin \alpha_0 / 2$, its value increases rapidly. This situation is seen from Fig. 2 for $\tan \beta = 50$. Thus, we may easily expect the value as large as 0.05. In order to obtain $|V_{13}|$, we have to multiply m_3/m_1 which may push its value larger, if $m_3 > m_1$.

(c) The induced Dirac CP violation phase δ

The induced Dirac CP violation phase contains β_0 which is not fixed in this model. Therefore, in general, the Dirac phase can take any value, until we fix the value of β_0 . In order to estimate the Dirac phase aside from β_0 , we define δ_1 given in Eq. (29), which

is obtained by excluding β_0 . With $\tan\beta = 50$, we show in Fig. 3, values of $\sin\delta_1$ in the $\sin^2 2\theta_{12}$ and m_1 plain. The solid line shows a curve on which $\sin\delta_1$ takes a fixed value. In the right-half domain, the larger value is obtained. As we stated, if α_0 enters in the domain $-\pi \leq \alpha_0 \leq 0$, the sign of $\sin\delta_1$ changes.

(d) The effective mass of the neutrinoless double beta decay $\langle m_\nu \rangle$

The model predicts the effective mass of order 0.05 eV as we see from Fig. 3 for $\tan\beta = 50$. The effective mass $\langle m_\nu \rangle$ is proportional to m_1 as shown in Eq. (30), it becomes larger as m_1 increases, while decreases if $\sin^2 2\theta_{12}$ increases.

All corresponding figures for $\tan\beta = 20$ are shown in Figs. 4, 5, 6. Except for $\langle m_\nu \rangle$, the figures are obtained by shifting the larger m_1 , because the dependence of $\tan\beta$ is scaled by ϵm_1^2 as we can see from the definition of h in Eq. (24). The effective mass $\langle m_\nu \rangle$ is almost the same as the case of $\tan\beta = 50$.

5. SUMMARY AND DISCUSSIONS

In this paper, we discuss a class of neutrino mass matrix which predicts zero or a small value of $|V_{13}|$ and found the inequality in Eq. (28). This constraint gives a severe restriction for model building of neutrino mass matrix. In particular, the model which predicts a larger value of $\tan^2\theta_{12}$ at M_R scale than the experimental value obtained from the solar neutrino mixing is excluded. As a result, the bi-maximal mixing scheme at M_R scale is excluded, if the experimental value $\tan^2\theta_\odot < 1$ is established.

In this model, $|V_{13}|$ in Eq. (19) at m_Z is induced radiatively and turns out to be not small as it is shown in Fig.2, if the neutrino mass m_1 is of order 0.05 eV. The Dirac phase δ_1 in Eq. (29) at m_Z is also induced and is not small in general as we see in Fig.3. The effective neutrino mass $\langle m_\nu \rangle$ in Eq. (30) is expected to be of order 0.05 eV. All these values for $|V_{13}|$, δ_1 and $\langle m_\nu \rangle$ depend crucially on the mass m_1 which is assumed to be around 0.05 eV.

The fact that Majorana phases at M_R scale can induce a Dirac phase pushes our dream further to consider the possible relation between a Dirac phase which appears in the neutrino oscillations and the Majorana phase which appears in the leptogenesis.

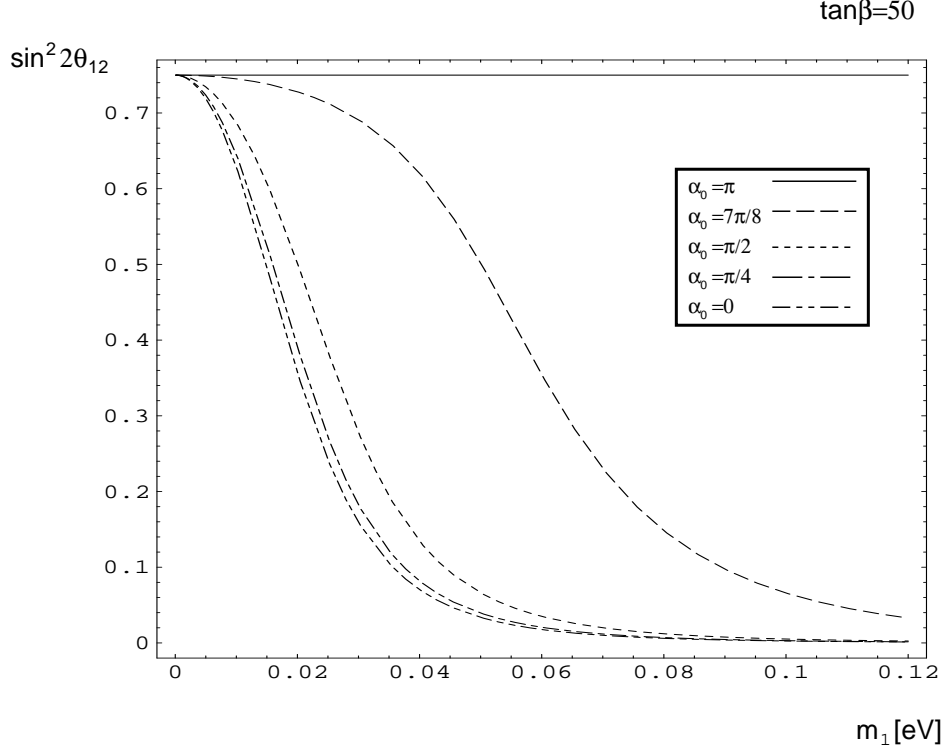


FIG. 1: Contour plot of α_0 in $\sin^2 2\theta_{12}$ and m_1 plane to reconstruct the experimental value of θ_\odot in the case of $\tan \beta = 50$. We use as experimental values $\tan^2 \theta_\odot = 0.34$ ($\sin^2 2\theta_\odot \simeq 0.75$), $\Delta m_\odot^2 = 5 \times 10^{-5} [\text{eV}^2]$, $\sin^2 2\theta_{\text{atm}} = 1$, and $\Delta m_{\text{atm}}^2 = 3 \times 10^{-3} [\text{eV}^2]$. The allowed region is between $\alpha_0 = \pi$ and $\alpha_0 = 0$ curves.

We believe such scenario does exist and the finding of the missing link will be the most wonderful and fruitful project.

Acknowledgment This work is supported in part by the Japanese Grant-in-Aid for Scientific Research of Ministry of Education, Science, Sports and Culture, No.12047218.

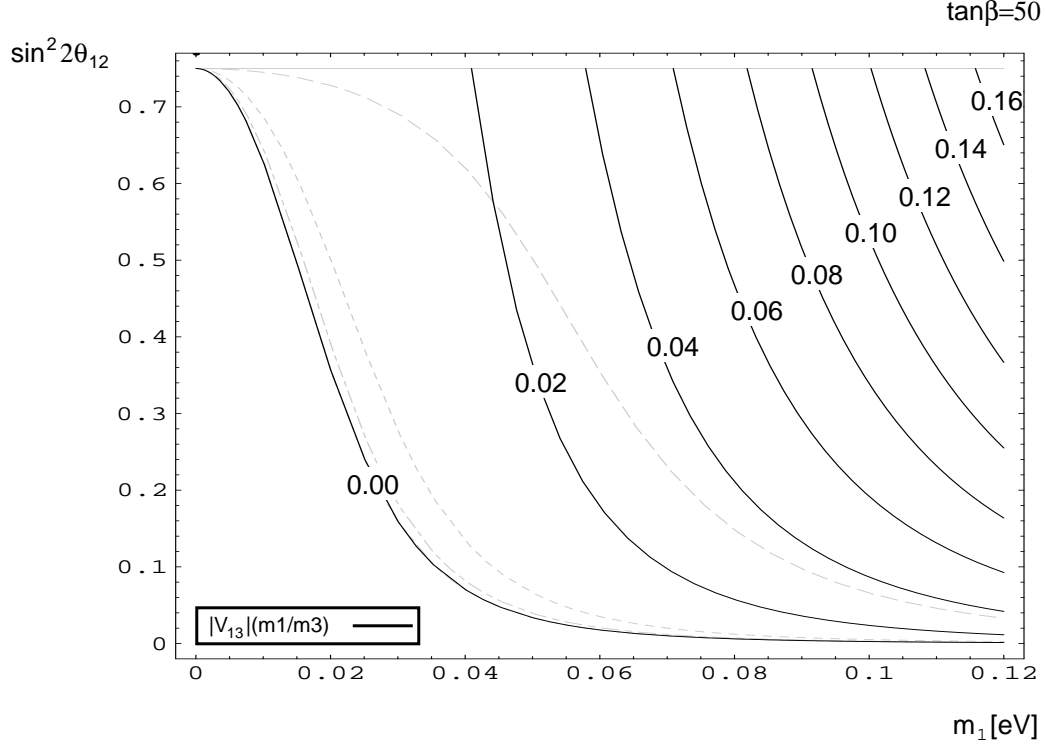


FIG. 2: Contour plot of $|V_{13}|(m_1/m_3)$ in $\sin^2 2\theta_{12}$ and m_1 plane for $\tan\beta = 50$. We use same values as Fig. 1 for experimental values. Gray curves show the α_0 values as in Fig. 1.

Appendix A: Diagonalization of the neutrino mass matrix

We define $\text{diag}(1, 1, \alpha)O = OX$,

$$\begin{aligned} X &= 1 - \epsilon O^T \text{diag}(0, 0, 1)O \\ &= 1 - \epsilon \begin{pmatrix} s_{12}^2 s_{23}^2 & s_{12} c_{12} s_{23}^2 & s_{12} s_{23} c_{23} \\ s_{12} c_{12} s_{23}^2 & c_{12}^2 s_{23}^2 & c_{12} s_{23} c_{23} \\ s_{12} s_{23} c_{23} & c_{12} s_{23} c_{23} & c_{23}^2 \end{pmatrix}, \end{aligned} \quad (\text{A.1})$$

where $\epsilon = 1 - \alpha$ is a small positive quantity and its value is given in Eq. (8), then we consider the mass matrix transformed by O as

$$\bar{m}_\nu \equiv O^T m_\nu(m_Z) O = X D_\nu X^T. \quad (\text{A.2})$$

Now, we diagonalize \bar{m}_ν .

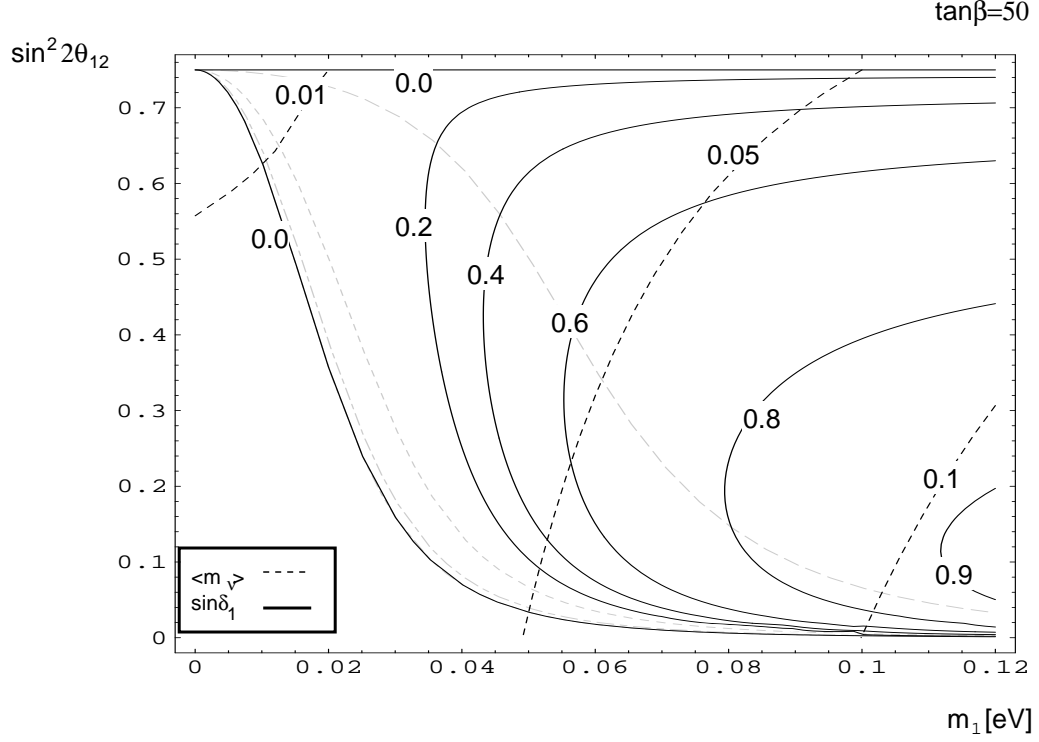


FIG. 3: Contour plot of $\sin\delta_1$ and $\langle m_\nu \rangle$ for $\tan\beta = 50$. We use same values as Fig. 1 for experimental values. Solid curves denote $\sin\delta_1$ and dashed curves denote $\langle m_\nu \rangle$. Gray curves show the α_0 values as in Fig. 1.

In order to diagonalize this matrix directly, we consider the Hermite matrix $\bar{m}_\nu^\dagger \bar{m}_\nu$

$$\bar{m}_\nu^\dagger \bar{m}_\nu \simeq (1 - 4\epsilon s_{12}^2 s_{23}^2) M_1^2 + Y, \quad (\text{A.3})$$

where elements of Y are given up to the 1st order of ϵ as

$$\begin{aligned} Y_{11} &= 0, \quad Y_{22} = \tilde{\Delta}_{21}, \quad Y_{33} = \tilde{\Delta}_{31}, \\ Y_{12} &= Y_{21}^* = -2\epsilon s_{12} c_{12} s_{23}^2 (M_1^2 + M_2^2 + 2M_1 M_2 e^{i\alpha_0}) M_1^2, \\ Y_{13} &= Y_{31}^* = -\epsilon s_{12} s_{23} c_{23} (M_1^2 + M_3^2 + 2M_1 M_3 e^{i\beta_0}), \\ Y_{23} &= Y_{32}^* = -\epsilon c_{12} s_{23} c_{23} (M_2^2 + M_3^2 + 2M_2 M_3 e^{i(\beta_0 - \alpha_0)}). \end{aligned} \quad (\text{A.4})$$

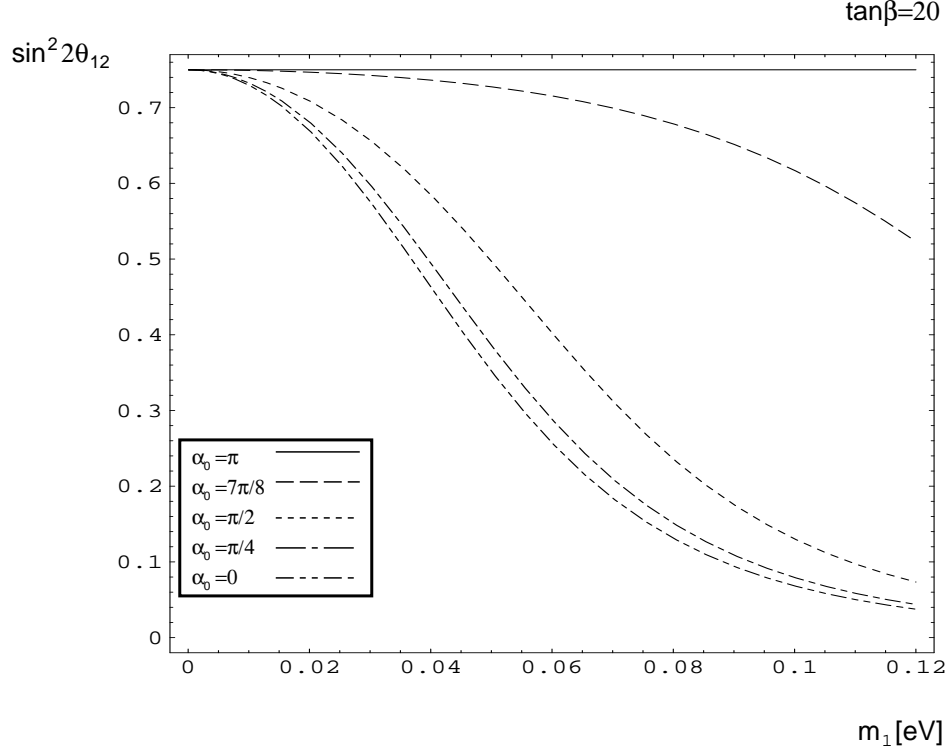


FIG. 4: Contour plot of α_0 in $\sin^2 2\theta_{12}$ and m_1 plane to reconstruct the experimental value of θ_\odot in the case of $\tan \beta = 20$. We use same values as Fig. 1 for experimental values. The allowed region is between $\alpha_0 = \pi$ and $\alpha_0 = 0$ lines.

$$\begin{aligned}\tilde{\Delta}_{21} &= \Delta_{21} - 4\epsilon s_{23}^2 (c_{12}^2 M_1^2 - s_{12}^2 M_2^2), \\ \tilde{\Delta}_{31} &= \Delta_{31} - 4\epsilon (c_{23}^2 M_3^2 - s_{12}^2 s_{23}^2 M_1^2).\end{aligned}\tag{A.5}$$

Since $\bar{m}_\nu^\dagger \bar{m}_\nu$ is an Hermite matrix, it is diagonalized by the unitary transformation as $V^\dagger \bar{m}_\nu^\dagger \bar{m}_\nu V \simeq (1 - 4\epsilon s_{12}^2 s_{23}^2) M_1^2 + V^\dagger Y V$. The diagonalization of the matrix Y can be achieved by using the see-saw technique, because $|Y_{33}|$ is much larger than all other terms. That is, by using the unitary matrix

$$V_3 \simeq \begin{pmatrix} 1 & 0 & \frac{Y_{13}}{Y_{33}} \\ 0 & 1 & \frac{Y_{23}}{Y_{33}} \\ -\frac{Y_{13}^*}{Y_{33}} & -\frac{Y_{23}^*}{Y_{33}} & 1 \end{pmatrix}.\tag{A.6}$$

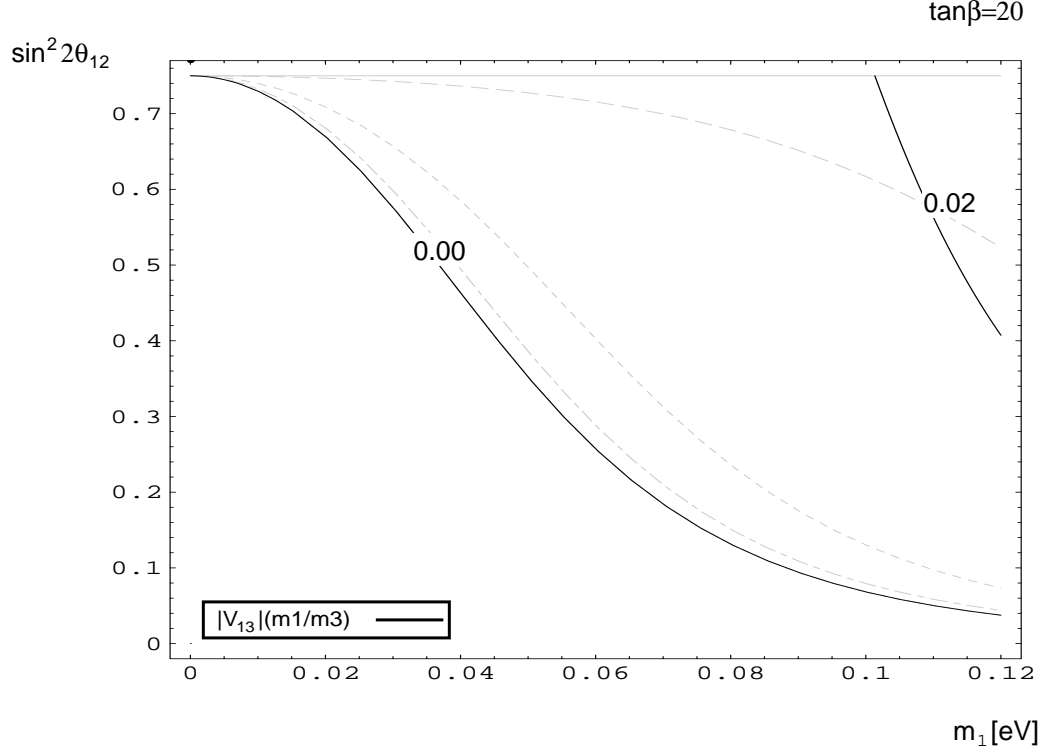


FIG. 5: Contour plot of $|V_{13}|(m_1/m_3)$ in $\sin^2 2\theta_{12}$ and m_1 plain for $\tan\beta = 20$. We use same values as Fig. 1 for experimental values. Gray curves show the α_0 values as in Fig. 4.

Y is block diagonalized in a good accuracy as

$$\begin{aligned}
 V_3^\dagger Y V_3 &\simeq \begin{pmatrix} -\frac{2|Y_{13}|^2}{Y_{33}} & Y_{12} - \frac{2Y_{13}Y_{23}^*}{Y_{33}} & 0 \\ Y_{12}^* - \frac{2Y_{13}^*Y_{23}}{Y_{33}} & Y_{22} - \frac{2|Y_{23}|^2}{Y_{33}} & 0 \\ 0 & 0 & Y_{33} + \frac{|Y_{13}|^2 + |Y_{23}|^2}{Y_{33}} \end{pmatrix} \\
 &\simeq \begin{pmatrix} 0 & Y_{12} & 0 \\ Y_{12}^* & Y_{22} & 0 \\ 0 & 0 & Y_{33} \end{pmatrix}, \tag{A.7}
 \end{aligned}$$

where in the last equation, we neglected the see-saw induced terms because $|Y_{13}/Y_{33}|$ and $|Y_{23}/Y_{33}|$ are much smaller than 1 and Y_{13} and Y_{23} are same order of Y_{12} and Y_{22} .

In the following, we use $M_1 = M_2$ for terms proportional to ϵ to simplify the expression.

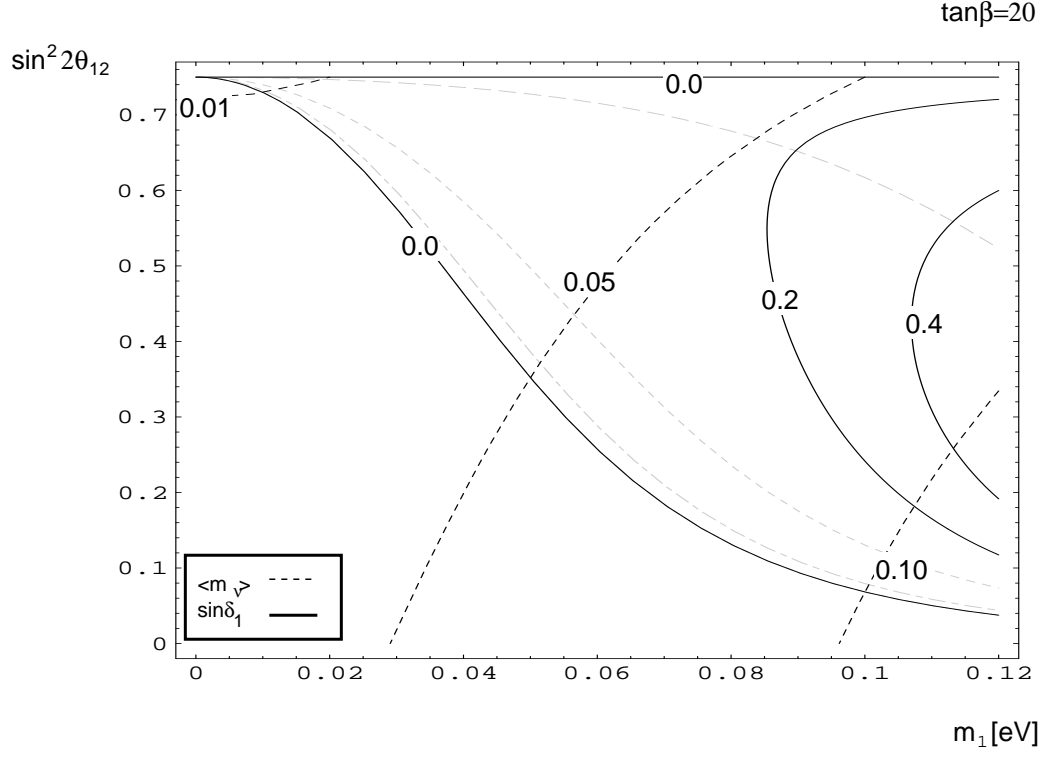


FIG. 6: Contour plot of $\sin\delta_1$ and $\langle m_\nu \rangle$ for $\tan\beta = 20$. We use same values as Fig. 1 for experimental values. Solid curves denote $\sin\delta_1$ and dashed curves denote $\langle m_\nu \rangle$. Gray curves show the α_0 values as in Fig. 4.

The matrix in Eq. (A7) is diagonalized by

$$V_{12} = \begin{pmatrix} c & -se^{i\alpha_0/2} & 0 \\ se^{-i\alpha_0/2} & c & 0 \\ 0 & 0 & 1 \end{pmatrix}, \quad (\text{A.8})$$

with $c = \cos\theta$ and $s = \sin\theta$ as

$$V_{12}^\dagger (V_3^\dagger Y V_3) V_{12} = \text{diag}(\lambda_1, \lambda_2, \lambda_3), \quad (\text{A.9})$$

where

$$\tan 2\theta = \frac{4\epsilon M_1^2 \sin 2\theta_{12} s_{23}^2 \cos \frac{\alpha_0}{2}}{\tilde{\Delta}_{21}}, \quad (\text{A.10})$$

and

$$\lambda_1 \simeq \frac{\tilde{\Delta}_{21}}{2} \left(1 - \frac{1}{\cos 2\theta} \right), \quad \lambda_2 \simeq \frac{\tilde{\Delta}_{21}}{2} \left(1 + \frac{1}{\cos 2\theta} \right), \quad \lambda_3 \simeq \tilde{\Delta}_{31}. \quad (\text{A.11})$$

Neutrino masses at m_Z are obtained by $m_i^2 = (1 - 4\epsilon s_{12}^2 s_{23}^2) M_1^2 + \lambda_i$ and

$$\begin{aligned} \Delta m_{\odot}^2 &\equiv m_2^2 - m_1^2 = \frac{\tilde{\Delta}_{21}}{\cos 2\theta}, \\ \Delta m_{\text{atm}}^2 &\equiv m_3^2 - m_2^2 \simeq m_3^2 - m_1^2 \simeq \tilde{\Delta}_{31}. \end{aligned} \quad (\text{A.12})$$

We find that the angle θ is expressed by

$$\sin 2\theta = \frac{4\epsilon M_1^2 \sin 2\theta_{12} s_{23}^2 \cos \frac{\alpha_0}{2}}{\Delta m_{\odot}^2}. \quad (\text{A.13})$$

By taking into account of

$$(OV_3 V_{12})^T m_{\nu}(m_Z) OV_3 V_{12} \simeq \text{diag}(m_1, m_2 e^{i\alpha_0}, m_3 e^{i\beta_0}), \quad (\text{A.14})$$

with $m_i > 0$, we find the mixing matrix V which satisfies $V^T m_{\nu}(m_Z) V = \text{diag}(m_1, m_2, m_3)$ is $V \equiv OV_3 V_{12} \text{diag}(1, e^{-i\alpha_0/2}, e^{-i\beta_0/2})$ is given by

$$V \simeq \begin{pmatrix} c_{12}c - s_{12}s e^{-i\alpha_0/2} & -(s_{12}c + c_{12}s e^{i\alpha_0/2}) & -|V_{13}|e^{i\rho} \\ c_{23}(s_{12}c + c_{12}s e^{-i\alpha_0/2}) & c_{23}(c_{12}c - s_{12}s e^{i\alpha_0/2}) & -s_{23} \\ s_{23}(s_{12}c + c_{12}s e^{-i\alpha_0/2}) & s_{23}(c_{12}c - s_{12}s e^{i\alpha_0/2}) & c_{23} \end{pmatrix} \begin{pmatrix} 1 & 0 & 0 \\ 0 & e^{-i\alpha_0/2} & 0 \\ 0 & 0 & e^{-i\beta_0/2} \end{pmatrix}, \quad (\text{A.15})$$

where

$$\begin{aligned} |V_{13}| &= \frac{\epsilon m_1 m_3 \sin 2\theta_{12} \sin 2\theta_{23} \sin \frac{\alpha_0}{2}}{\tilde{\Delta} m_{31}^2}, \\ \rho &= \frac{\pi}{2} - \frac{\alpha_0}{2} + \beta_0. \end{aligned} \quad (\text{A.16})$$

-
- [1] Y. Fukuda *et al.* [Super-Kamiokande Collaboration], Phys. Rev. Lett. **81**, 1562 (1998).
 - [2] Q. R. Ahmad *et al.* [SNO Collaboration], Phys. Rev. Lett. **87**, 071301 (2001); Q. R. Ahmad *et al.* [SNO Collaboration], arXiv:nucl-ex/0204009.
 - [3] S. Fukuda *et al.* [SuperKamiokande Collaboration], Phys. Rev. Lett. **86**, 5651 (2001).
 - [4] A. de Gouvea, A. Friedland and H. Murayama, Phys. Lett. B **490**, 125 (2000).
 - [5] C. Bemporad [Chooz Collaboration], Nucl. Phys. Proc. Suppl. **77**, 159 (1999); M. Apollonio *et al.* [CHOOZ Collaboration], Phys. Lett. B **466**, 415 (1999).
 - [6] Z. Maki, M. Nakagawa and S. Sakata, Prog. Theor. Phys. **28**, 870 (1962).
 - [7] S. M. Bilenky, J. Hosek and S. T. Petcov, Phys. Lett. B **94**, 495 (1980).
 - [8] M. Doi, T. Kotani, H. Nishiura, K. Okuda and E. Takasugi, Phys. Lett. B **102**, 323 (1981).
 - [9] J. Schechter and J. W. Valle, Phys. Rev. D **22**, 2227 (1980); Phys. Rev. D **23**, 1666 (1981).
 - [10] F. Vissani, arXiv:hep-ph/9708483; V. D. Barger, S. Pakvasa, T. J. Weiler and K. Whisnant, Phys. Lett. B **437**, 107 (1998); A. J. Baltz, A. S. Goldhaber and M. Goldhaber, Phys. Rev. Lett. **81**, 5730 (1998).
 - [11] H. Harari, H. Haut and J. Weyers, Phys. Lett. B **78**, 459 (1978); Y. Koide, Phys. Rev. D **39**, 1391 (1989); H. Fritzsch and Z. Z. Xing, Phys. Lett. B **372**, 265 (1996); M. Fukugita, M. Tanimoto and T. Yanagida, Phys. Rev. D **57**, 4429 (1998).
 - [12] N. Cabibbo, Phys. Lett. B **72**, 333 (1978); L. Wolfenstein, Phys. Rev. D **18**, 958 (1978); V. D. Barger, K. Whisnant and R. J. Phillips, Phys. Rev. D **24**, 538 (1981); A. Acker, J. G. Learned, S. Pakvasa and T. J. Weiler, Phys. Lett. B **298**, 149 (1993); R. N. Mohapatra and S. Nussinov, Phys. Lett. B **346**, 75 (1995); P. F. Harrison, D. H. Perkins and W. G. Scott, Phys. Lett. B **349**, 137 (1995); Phys. Lett. B **374**, 111 (1996); Phys. Lett. B **396**, 186 (1997); Phys. Lett. B **458**, 79 (1999); C. Giunti, C. W. Kim and J. D. Kim, Phys. Lett. B **352**, 357 (1995); R. Foot, R. R. Volkas and O. Yasuda, Phys. Lett. B **433**, 82 (1998).
 - [13] K. Fukuura, T. Miura, E. Takasugi and M. Yoshimura, Phys. Rev. D **61**, 073002 (2000).
 - [14] N. Haba and N. Okamura, Eur. Phys. J. C **14**, 347 (2000); T. Miura, E. Takasugi and

- M. Yoshimura, Prog. Theor. Phys. **104**, 1173 (2000).
- [15] J. A. Casas, J. R. Espinosa, A. Ibarra and I. Navarro, JHEP **9909**, 015 (1999); Nucl. Phys. B **573**, 652 (2000); K. R. Balaji, A. S. Dighe, R. N. Mohapatra and M. K. Parida, Phys. Rev. Lett. **84**, 5034 (2000); N. Haba, Y. Matsui, N. Okamura and T. Suzuki, Phys. Lett. B **489**, 184 (2000).
- [16] N. Haba, Y. Matsui and N. Okamura, Eur. Phys. J. C **17**, 513 (2000); N. Haba, Y. Matsui, N. Okamura and M. Sugiura, Prog. Theor. Phys. **103**, 145 (2000).